Dynamic and Equilibrium Studies on the Interaction of Ran with Its Effector, RanBP1[†]

Jürgen Kuhlmann,*[,‡] Ian Macara,[§] and Alfred Wittinghofer[‡]

Max-Planck-Institut für molekulare Physiologie, Rheinlanddamm 201, 44139 Dortmund, Germany, and Center of Cell Signaling, Health Sciences Center, University of Virginia, Charlottesville, Virginia 22908

Received March 6, 1997; Revised Manuscript Received August 1, 1997[⊗]

ABSTRACT: Ran, a small nuclear GTP-binding protein, is one of the most abundant Ras-related proteins in eucaryotic cells. Ran is essential for nucleo−cytoplasmatic transport and is primarily localized in the nucleus and at the nuclear pore complex. Here, we characterize the kinetics and equilibrium of the interaction between Ran and RanBP1 by two independent biophysical approaches: fluorescence spectroscopy using analogues of guanine nucleotides and surface plasmon resonance in the BIAcore system. Both approaches result in kinetic and equilibrium data which are in good agreement with each other. Affinities of RanBP1 for Ran in the GTP-bound state were in the nanomolar range, while Ran·GDP bound RanBP1 with a dissociation constant around 10 μM. Interestingly, the difference in affinity of RanBP1 for Ran·GDP was mostly due to a dramatic increase of the dissociation rate constant. Mutant Ran protein lacking the last five amino acids of the C-terminus (RanΔC) is unable to facilitate nuclear import *in vitro* and does not bind to RanBP1. Here, we show that RanBP1 binds RanΔC·mGppNHp with K_D values around 10 μM, as is the case for its association with full-length Ran·GDP. The loss of affinity of RanBP1 for the triphosphate form of RanΔC was a result of both a decrease of the association rate and a moderately increased dissociation of the RanΔC·RanBP1 complex. Circular dichroism spectra indicate significant changes in the secondary structure of either Ran·GppNHp, RanBP1, or both proteins upon forming a stable complex with each other.

First cloned from a human teratocarcinoma cDNA library, Ran[1] encodes a 216 amino acid GTP-binding protein of 24 kDa, representing a distinct, highly conserved subfamily within the superfamily of Ras-related GTP-binding proteins (Macara et al., 1996). While the discovery of Ran was initially correlated with a suggested role in cell cycle regulation (Ren et al., 1994; Kornbluth et al., 1994), the focus of interest has now shifted to the function of Ran in nucleo−cytoplasmic transport [for a review, see Rush et al. (1996), Moore and Blobel (1994), Sazer (1996), Görlich and Mattaj (1996), Melchior et al. (1995), and Schlenstedt (1996)].

Like all Ras-related GTP-binding proteins, Ran cycles between a GTP- and a GDP-bound state. While the spontaneous conversion between these two states is very sluggish as Ran binds guanine nucleotides very tightly (Klebe et al., 1993) and hydrolyzes GTP very slowly (Bischoff et al., 1994), the dissociation of Ran-bound GDP is increased 10^6-fold by RCC1, a nuclear protein which represents the nucleotide exchange factor of Ran (Klebe et al., 1995b). Likewise, the rate of GTP hydrolysis by Ran is increased 10^5-fold by RanGAP1, the GTPase activating protein for Ran (Klebe et al., 1995a).

In contrast to Ras and many Ras-related proteins, Ran is not posttranslationally modified at its C-terminus. Instead, the C-terminal end of Ran is characterized by a distinctive sequence of acidic amino acids (DEDDDL), which is conserved in all Ran homologous proteins and appears to be essential for the function of Ran. Analogous to Ras, the GTP-bound form of Ran is recognized by a number of putative effector proteins. Ran binding protein 1 (RanBP1) was identified and cloned by probing renatured blot overlays of human (HeLa) and hamster (tsBN2) cell extracts with Ran·[γ-^{32}P]GTP (Coutavas et al., 1993). RanBP1 has an apparent molecular mass of 27 kDa and is 98% identical with the mouse HTF9a cDNA, which was discovered in a search for bidirectional promoters (Bressan et al., 1994). RanBP1 consists of 203 amino acids, is highly charged (about 40% Arg, Asp, Glu, Lys) with a prevalence of acidic residues, and contains 2 regions homologous to the consensus sequence of a coiled-coil. Database analysis (Hartmann & Görlich, 1995) and blot overlay assays with cell lysates or yeast double-hybrid systems revealed additional Ran·GTP-binding proteins with apparent molecular masses above 100 kDa (Lounsbury et al., 1994; Bischoff et al., 1995; Beddow et al., 1995). Another target of Ran, RanBP2, was identified as an element of the nuclear pore complex (Yokoyama et al., 1995).

So far, several studies have been carried out to characterize the interaction between RanBP1, Ran, and its regulators (RCC1 and RanGAP) (Bischoff et al., 1995; Beddow et al., 1995; Ren et al., 1995). Filter-binding assays, double-hybrid

[†] This work was supported by HFSP Grant RG-423/95.

* Corresponding author.

[‡] Max-Planck-Institut für molekulare Physiologie.

[§] University of Virginia.

[⊗] Abstract published in *Advance ACS Abstracts,* September 15, 1997.

[1] Abbreviations: DTE, dithioerythritol; GAP: GTPase activating protein; GST, glutathione *S*-transferase; mantGxP, mGxP, 2′,3′-bis-*O*-(methylanthraniloyl)guanosine di- (D), tri- (T), or 5′-(β,γ-imidotri)-(ppNHp) phosphate, mixture of 2′/3′-isomers; mantdGDP, mdGDP, 2′-desoxy-3′-*O*-(methylanthraniloyl)guanosine diphosphate; GppNHp, guanosine-5′-(β,γ-imidotriphosphate); Ran, Ras like nuclear protein product of the human gene Ran/TC4; RanΔC, wild-type Ran protein lacking the C-terminal DEDDDL sequence; RanBP, Ran-binding protein; RCC1, regulator of chromosome condensation; SDS, sodium dodecyl sulfate; SPR, surface plasmon resonance.

S0006-2960(97)00524-2 CCC: $14.00

systems, and chromatographic methods indicated that RanBP1 strongly binds to Ran·GTP but not to Ran·GDP (Coutavas et al., 1993) and enhances the GTPase-stimulating effect of RanGAP on Ran·GTP (Bischoff et al., 1995). Specific recognition of Ran by RanBP1 is dependent on the Ran C-terminal sequence (Ren et al., 1995). Few data are available describing the interaction between Ran and Ran·GTP-binding proteins in quantitative terms. Due to the fact that at least two classes of proteins, RanBP1/RanBP2 and importin-β, are able to bind Ran·GTP simultaneously (Görlich et al., 1996), detailed knowledge about the dynamics of the interaction between Ran and its effectors is necessary in order to understand the crucial steps in import and export through the nuclear pore. Therefore, we were interested to obtain biophysical information about the kinetics and equilibria of the Ran−RanBP1 interaction. The results presented here contribute to a further understanding of protein−protein interactions during nucleo−cytoplasmic transport and the role of Ran therein.

MATERIALS AND METHODS

Proteins and Nucleotides. $p24^{Ran}$ (simply Ran) was expressed in a pET3d vector using *E. coli* BL21 as described previously (Klebe et al., 1993). To prevent the strong tendency of Ran to form oligomers at high concentrations (Plass, unpublished results), cells were disintegrated in a laboratory mill (BIOmatik) with glass beads (i.d. 0.1 mm). The cell lysate was filtered and applied to an ion-exchange column (Fractogel EMD SO_3-650S, Merck) after centrifugation. Ran protein was bound to the column in 20 mM KP_i, pH 6.4, 6.5 mM DTE, 5 mM $MgCl_2$, and 10 μM GDP and eluted with a 0−1 M KCl gradient using 8 column volumes at 2 mL/min. The Ran fraction was collected and precipitated by 3 M (w/v) $(NH_4)_2SO_4$. The protein was dissolved in KP_i buffer (see above, but pH 7.4) and shock-frozen. Ran could be isolated by this procedure in >95% purity as analyzed by SDS gel electrophoresis.

RanBP1 was expressed in a pET11d vector using *E. coli* BL21. Cells were disintegrated in a laboratory glasmill as described for Ran, and the soluble part of the cell lysate was purified on a DEAE column (elution: 0−1 M NaCl gradient). The fractions containing RanBP1 were collected, and protein was precipitated by ammonium sulfate and dissolved in 30 mM Tris-HCl, pH 7.4, 300 mM NaCl, and 1 mM DTE. Using the same buffer, RanBP1 was applied to a Superdex G200 gel filtration column, yielding RanBP1 of purity about >95% as analyzed by SDS gel electrophoresis. GST fusion proteins, cloned in pGEX vectors (Pharmacia), were expressed from *E. coli* BL21, which were induced (10−100 μM IPTG) and incubated overnight at 30 °C. After harvesting, cells were lysed by sonication and purified over a glutathione−Sepharose column.

Proteins were stored in a concentrated form (>2 mg/mL) at −80 °C over a period of 6 months in KP_i-buffer (20 mM KP_i, pH 7.4, 6.5 mM DTE, and 5 mM $MgCl_2$) without loss of activity. Loading of Ran with nucleotides other than GDP was performed as described by Klebe et al. (1995a), separation of protein and free ligand took place on a HighTrap gel filtration column (Pharmacia), and loading efficiency was analyzed by HPLC.

For fluorescence studies, *N*-methylanthraniloyl (mant) derivatives of GDP, GTP, GppNHp, and the corresponding deoxynucleotides were prepared as described by Hiratsuka (1983) and John et al. (1990). The products of synthesis were purified by ion-exchange chromatography on Q-Sepharose (1.8 × 15 cm) with a gradient of 0.2−0.6 M triethylammonium bicarbonate. Concentrations were determined spectroscopically for nucleotides and by using the standard method described by Bradford (1976) for proteins.

All solutions were degassed and filtered before use in fluorescence assays.

Biophysical Analysis. (i) Equilibria and Slow Kinetics Using Fluorescent Probes. Emission and excitation spectra of fluorescent probes were obtained from a Perkin Elmer (LS50B) or a SPEX Fluoromax fluorescence spectrometer. Titration experiments were performed using the Fluoromax spectrometer combined with a Model 22 infusion pump (Harvard Apparatus) and a house-built injection system and control software (HUBTIT).

Slow dissociation experiments were analyzed using GRAFIT 3.0 software, and titration data were fitted using SCIENTIST 2.0 software. Three buffer systems were used for dissociation reactions: Tris: 64 mM Tris-HCl, pH 7.6, 5 mM $MgCl_2$, and 1 mM DTE; KP_i: 20 mM KP_i, pH 7.5, 5 mM $MgCl_2$, and 1 mM β-mercaptoethanol; HEPES: 10 mM HEPES, pH 7.4, 5 mM $MgCl_2$, 0.0005% (w/v) Igepal, and 150 mM NaCl.

(ii) Fast Kinetics Using Fluorescent Probes. Association kinetics with Ran·mGXP were measured in a SX16MV stopped flow system (Applied Photophysics) under pseudo-first-order conditions and analyzed using the Applied Photophysics software. Excitation of the fluorophore was performed at 350 nm, and the emission signal was measured using a cutoff filter, KV408 (Schott).

Complex formation between proteins A (Ran) and B (RanBp1) is described by

$$\frac{d[AB]}{dt} = k_{on}[A][B] - k_{off}[AB] \quad (1.1)$$

Replacing [A], the concentration of A at time t, by $[A_0] - [AB]$, where $[A_0]$ = the concentration of A at $t = 0$, leads to

$$\frac{d[AB]}{dt} = k_{on}([A_0] - [AB])[B] - k_{off}[AB] \quad (1.2)$$

and

$$\frac{d[AB]}{dt} = k_{on}[B][A_0] - (k_{on}[B] + k_{off})[AB] \quad (1.3)$$

If $[B_0] \gg [A_0]$, $k_{on}[B]$ can be replaced by k_{on}':

$$\frac{d[AB]}{dt} = k_{on}'[A_0] - (k_{on}' + k_{off})[AB] \quad (1.4)$$

Thus, a plot of $d[AB]/dt$ vs [AB] results in a straight line with a slope of $k_{on}' + k_{off}$. Due to $k_{on}' = k_{on}[B]$, a plot of $(k_{on}' + k_{off})$ vs [B] provides a line with slope k_{on} and ordinate k_{off}.

(iii) Surface Plasmon Resonance. Association and dissociation reactions involving Ran·GppNHp without any fluorescence label were studied by surface plasmon resonance (SPR) in a BIAcore system (Pharmacia BIOsensor, Uppsala). To overcome partial inactivation of the immobilized ligand by reaction of essential lysine residues of the coupled protein,

we used a sandwich assay (Lenzen et al., in preparation) with anti-GST monoclonal antibody GST(12) (IC Chemicals) or anti-GST-sera (Pharmacia BIOsensor, Uppsala), which was coupled following the standard coupling protocol of the manufacturer (O'Shannessy et al., 1992). GST proteins were incubated at a concentration of 0.2 g/L for 7 min, following incubation with free ligand (control for nonspecific binding to the anti-GST surface). Regeneration with 20 mM glycine, pH 2, and 0.005% SDS resulted in complete dissociation of all noncovalently bound ligands, leaving the immobilized immunoglobulin at approximately full activity.

Binding of Ran to binary complexes of antibody and GST−RanBP1 was analyzed in a concentration-dependent manner using BIAlogue 2.1 evaluation software. To eliminate the contribution of nonspecific binding, equivalent controls with Ran·GDP were used to calculate specific signal changes if necessary. Experiments were performed in 10 mM HEPES, pH 7.4, 5 mM $MgCl_2$, and 0.0005% (w/v) Igepal CA-630 (Sigma) as a buffer system stabilizing the immobilized anti-GST antibodies.

(iv) Circular Dichroism Spectroscopy. Circular dichroism spectra were recorded at 20 °C using 2 mm cuvettes (Hellma, 121.000 QS) in a Jasco J710 CD-spectrometer calibrated with (+)-camphor-10-sulfonic acid. The bandwidth was 1 nm, rate of scanning 50 nm/min, and response time 1 s. Buffer conditions were 10 mM KP_i, pH 7.4, 5 mM $MgCl_2$. No β-mercaptoethanol or DTE was used to reduce absorbance in the UV range. Netto spectra were calculated by subtracting buffer spectra using EXCEL 5.0 software.

RESULTS

The interaction between Ran and its putative downstream effectors has so far only been studied by qualitative or at best semiquantitative methods. To obtain reliable quantitative information, we established two independent techniques for kinetic and equilibria studies.

Fluorescence Assays. Ran, like other GTPases of the Ras superfamily, exhibits a high affinity for GDP and GTP. Fluorescent analogues of these guanine nucleotides have been used to characterize nucleotide binding and exchange on Ran, taking advantage of the changes in fluorescence yield of the fluorescent (mant- or m-) group in aqueous and protein environments (Klebe et al., 1995a,b). To study the interaction of Ran with ranBP1, the fluorescently labeled, noncleavable GTP analogue mGppNHp was used instead of mGTP in most experiments to prevent mGTP hydrolysis by the intrinsic, albeit slow, GTPase activity of Ran.

In contrast to Ras, saturation of Ran·mGppNHp with RanBP1 gives a direct fluorescence readout resulting in an approximately 1.5-fold increase of the fluorescence signal (Figure 1). The fluorescence increase can be reversed by adding excess nonlabeled Ran·GppNHp. This can be used to determine the dissociation rate of the complex, which is sufficiently slow to be observed in a fluorescence spectrometer (Figure 2). As Ran is unstable above 20 °C over longer time periods, all measurements were performed at 20 °C. In addition, we observed that RanBP1 stabilizes the fluorescence signal of Ran·mGppNHp, probably by preventing its denaturation. Since all our SPR experiments (BIAcore, see below) are done with GST−RanBP1 fusion proteins, some of the fluorescence studies were done with both RanBP1 and GST−RanBP1 to measure the effect, if any, of the GST moiety. Dissociation rate constants for RanBP1 and GST−RanBP1 are roughly identical and increase with the ionic strength of the buffer system (Table 1).

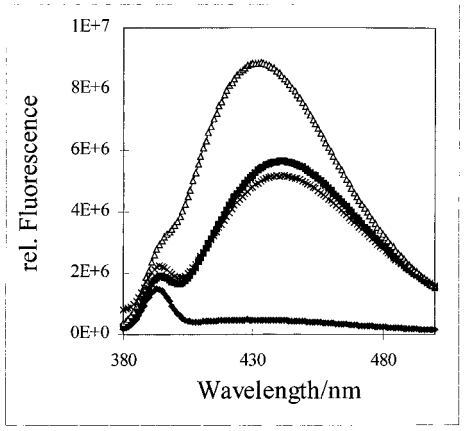

FIGURE 1: Emission spectra of Ran·mGppNHp. Fluorescence emission spectra of 200 nM Ran·mGppNHp was measured before (■) and after addition of 400 nM RanBP1 (△). A 50-fold excess of Ran·GppNHp (×) added to the probe resulted in a decrease of the fluorescence signal, which is just below the starting Ran·mGppNHp level due to dilution. Buffer control (◆) shows the Raman signal. Experiments were carried out in 64 mM Tris-HCl, pH 7.6, 5 mM $MgCl_2$, and 1 mM DTE at 20 °C, excitation at 350 nm.

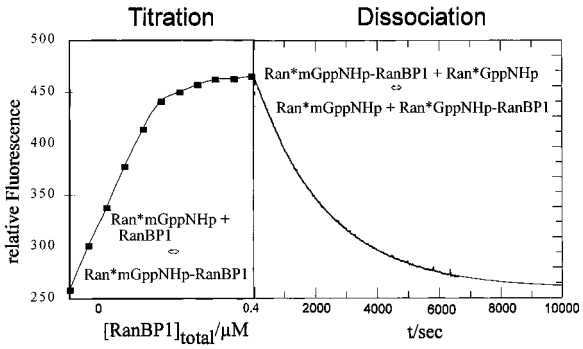

FIGURE 2: Binding of RanBP1 to Ran·mGppNHp and dissociation of the Ran·mGppNHp−RanBP1 complex after adding excess Ran·GppNHp. 200 nM Ran·mGppNHp (in 64 mM Tris-HCl, pH 7.6, 5 mM $MgCl_2$, and 1 mM DTE) was titrated with RanBP1 protein (stock solution 132 μM), while the fluorescence signal at 440 nm was monitored (excitation at 350 nm). Adding a 50-fold excess of nonlabeled Ran·GppNHp to the mixture decreased the fluorescence signal due to competition with Ran·mGppNHp. All data were collected in a SPEX Fluoromax fluorescence spectrometer at 20 °C, taking advantage of a house-built titrator apparatus and the timebase module of the DATAMAX software. Data of the dissociation reaction were processed in EXCEL and fitted as first-order exponentials in GRAFIT ($k_{off} = 4.3 \times 10^{-4}$ s^{-1}).

Experiments using overlay assays (Lounsbury et al., 1994) or the yeast two-hybrid interaction system (Ren et al., 1995) pointed out that RanBP1 does not bind to RanΔC lacking the C-terminal DEDDDL sequence. We were interested in measuring the effect of the C-terminal truncation in solution. The dissociation rate for C-terminally truncated Ran·mGppNHp (RanΔC·mGppNHp) complexed with RanBP1 is very fast and difficult to measure in a fluorescence spectrometer, and becomes impossible to measure for the Ran·mGDP·RanBP1 complex. The dissociation reaction for RanΔC, as measured by the competition assay, is higher by about 2 orders of magnitude compared to full-length Ran, without any effect of buffer ionic strength. In order to be able to measure fast dissociation rate constants, we took

Table 1: Dissociation Rates for Complexes between RanBP1 and Ran Constructs[a]

Ran protein	RanBP	Tris	HEPES	KP_i
Ran·mGppNHp	RanBP1	4.3×10^{-4} [b]	10.7×10^{-4} [b]	$(2.8 \pm 0.4) \times 10^{-4}$, $n = 4$[b]
Ran·mGppNHp	GST−RanBP1	5.2×10^{-4} [b]	$(10.5 \pm 1.1) \times 10^{-4}$, $n = 4$[b]	3.7×10^{-4} [b]
Ran·2′d3′mGDP	RanBP1	0.35[c]	0.93[c]	0.18[c]
RanΔC·mGppNHp	RanBP1			0.0097[c]
				0.011[b]

[a] All measurements were performed at 20 °C with either a Perkin Elmer LS50B or a SPEX Fluoromax fluorescence spectrometer. Buffer systems: see Materials and Methods. [b] k_{off} determined in a competition experiment as described in Figure 3. [c] Off-rates were estimated from the ordinate value (k_{obs} vs [RanBP1]) of association experiments in an Applied Photophysics stopped-flow instrument (see below).

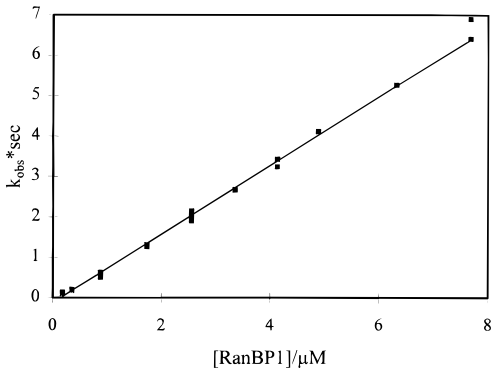

FIGURE 3: Association of RanBP1 with Ran·mGppNHp 200 nM Ran·mGppNHp (final concentration) was mixed with increasing concentrations of RanBP1 in a SX17MV stopped-flow instrument (Applied Photophysics). The excitation wavelength was 350 nm; fluorescence was observed using a cutoff filter (KV408). Kinetics were analyzed assuming pseudo-first-order conditions and the fitted k_{obs} values plotted against [RanBP1] (μM). Linear regression of these data resulted in a slope of 0.848 μM s^{-1} corresponding to a k_{on} of 8.5×10^5 M s^{-1}. All experiments were performed in 64 mM Tris-HCl, pH 7.6, 5 mM $MgCl_2$, and 1 mM DTE at 20 °C.

advantage of the fact that association reactions measured under pseudo-first-order conditions (see below) yield a linear relationship between the observed rate constant, k_{obs}, and the concentration of free ligand. The intercept with the ordinate of a plot k_{obs} vs [ligand] gives a value for k_{off}. Table 1 summarizes the results obtained for different combinations of proteins and buffer conditions. For RanΔC·mGppNHp, the dissociation rates from both stopped-flow experiments and fluorescence competition could be measured and were found to be in good agreement (about 0.01/s), demonstrating the validity of the two approaches.

Association rate constants for complex formation were obtained by stopped-flow experiments with a SX17MV system (Applied-Photophysics), recording the fluorescence increase after mixing different concentrations of RanBP1 with a constant amount of Ran·mGxP. Single exponential analysis yielded apparent rate constants for pseudo-first-order reactions, which were plotted as a function of free [RanBP1] to provide k_{on} for the second-order reaction (Figure 3). The method was used for high-affinity complexes formed by full-length Ran in the GTP-bound state and RanBP1, as well as for low-affinity complexes like those between RanBP1 and the C-terminal truncated RanΔC in the GTP-bound state or Ran in the GDP-bound state. In the latter cases, the dissociation of the complex could not be neglected in the analysis, and was in fact used to determine the dissociation rate constants shown in Table 1.

As summarized in Table 2, binding of RanBP1 and GST−RanBP1 to Ran in the GTP-bound state is a fast reaction with association rate constants on the order of 10^5−10^6/(M·s).

Table 2: Association Rates for Binding of Ran Proteins with RanBP1 at 20 °C[a]

Ran protein	RanBP	buffer	k_{on} [(M·s) × 10^{-5}]
Ran·mGppNHp	RanBP1	Tris	8.5
		HEPES	7.9
		KP_i	4.5
Ran·mGppNHp	GST−RanBP1	Tris	3.5
		HEPES	3.0
		KP_i	1.5
Ran·mGTP	RanBP1	KP_i	3.5
Ran·mGDP	RanBP1	KP_i	0.37
		Tris	0.64
Ran·2′d3′mGDP	RanBP1	HEPES	0.83
		KP_i	0.39
RanΔC·mGppNHp	RanBP1	KP_i	0.044

[a] k_{on} values were calculated according to Figure 5 from single-exponential fits of stopped-flow data. Off-rates were estimated from the ordinate value (k_{obs} vs [RanBP1]). For composition of buffers, see Materials and Methods.

In contrast to the dissociation reaction (where phosphate buffer with low ionic strength seemed to stabilize the complex), KP_i buffer now exhibits the slowest on-rate for the second-order reaction, while only small differences were found between Tris and HEPES buffer (ionic strength about 80 and 175, mM respectively). While no influence of the GST moiety was found on the dissociation reaction, the GST−RanBP1 fusion protein shows a 2−3-fold reduction in on-rate compared with RanBP1.

In contrast to the measurements of the dissociation rate, the association rate is sufficiently fast to allow using Ran·mGTP without interference from GTP hydrolysis. No significant difference is seen between the association rate constants of Ran·mGppNHp and Ran·mGTP. Assuming a similar finding for the dissociation reaction, we can expect that the interaction between Ran and RanBP1 is not influenced by the nature of the nucleoside triphosphate. Ran in the GDP-bound state (Ran·mGDP or Ran·mdGDP) has a 10-fold lower association rate constant for complex formation with RanBP1. While the effect of the di- vs triphosphate state in association is just 1 order of magnitude, the off-rate (calculated from the k_{obs} vs [RanBP1] plot) is increased by a factor of 10^3, whereas the dependence on the ionic strength of the buffer systems, as shown for the triphosphate experiments, remains unchanged. The association rate for binding of RanBP1 to RanΔC·mGppNHp is reduced 100-fold, without any significant effect of the buffer.

While the instability of Ran proteins *in vitro* at higher temperatures excluded long-term measurements above 20 °C, the short time range of stopped-flow experiments allowed us to study the temperature dependence of the association reaction between Ran·mGppNHp and RanBP1. Figure 4 shows the temperature dependence of the pseudo-first-order rate constant for the formation of the Ran·mGppNHp·RanBP1

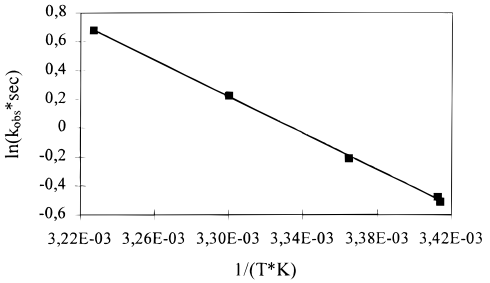

FIGURE 4: Temperature dependence of the association reaction between Ran·mGppNHp and RanBP1. Association of 1 μM RanBP1 with 200 nM Ran·mGppNHp was measured as described in Figure 5. Kinetics were fitted using first-order approximation and resulting rates for k_{obs} were plotted in a semilogarithmic plot as a function of $1/T$. Linear regression gives a value of 52 kJ/mol for E_A.

complex in an Arrhenius plot according to eq 2:

$$\nu = A \exp(-E_A/RT) \qquad (2)$$

The activiation energy, E_A, of the reaction was calculated by a least-squares fit to be 52 kJ/mol, which is a low energy barrier, close to the range of 30−40 kJ/mol typical for diffusion-controlled reactions (Gutfreund, 1995).

Using the dissociation and association rate constants, low affinities are calculated for the complexes of full-length Ran·GDP or RanΔC·GppNHp with RanBP1. To determine independent K_D values for those complexes, an automated fluorescence titration device was used. Assuming 1:1 stoichiometry, the dissociation constant K_D could be determined as described in Figure 5.

Table 3 gives an overview for equilibrium dissociation constants in the Ran−RanBP1 system based on kinetic and equilibria data for several combinations of Ran constructs and mant-labeled nucleotides, with a reasonable agreement between the two data sets. Both C-terminal truncated Ran protein in the GTP-bond (GppNHp-) state and full-length Ran in the GDP-bound state exhibit an approximately 10 000-fold reduced affinity for RanBP1, switching from the nanomolar to the micromolar range.

Surface Plasmon Resonance. While the fluorescence studies described here assume identical (or at least very similar) biochemical behavior of the endogenous ligand and its fluorescent derivative, solid-phase experiments based on plasmon surface resonance allow the use of nonlabeled nucleotides. Using a BIAcore instrument (VanCott et al., 1992; Malmborg et al., 1992; Chaiken et al., 1992), we show that the binding of Ran·GppNHp to immobilized RanBP1 can be observed directly.

Using the standard procedure suggested by the manufacturer, one reactant is immobilized via an amine coupling system to the carboxylated dextran matrix of the sensor chip surface. Depending on the availability of its lysine residues, coupling might result in complete or partial inactivation of the immobilized protein since these particular lysine(s) might be important for the interaction with the ligand in solution. To overcome this problem, indirect coupling of proteins has been suggested using NTA for binding His-tagged proteins (Gershon & Khilko, 1994) or anti-GST matrices for GST fusion proteins. Here we used a sandwich assay with anti-GST monoclonal antibody GST(12) (IC Chemicals) or anti-GST sera (Pharmacia BIOsensor, Uppsala) covalently bound

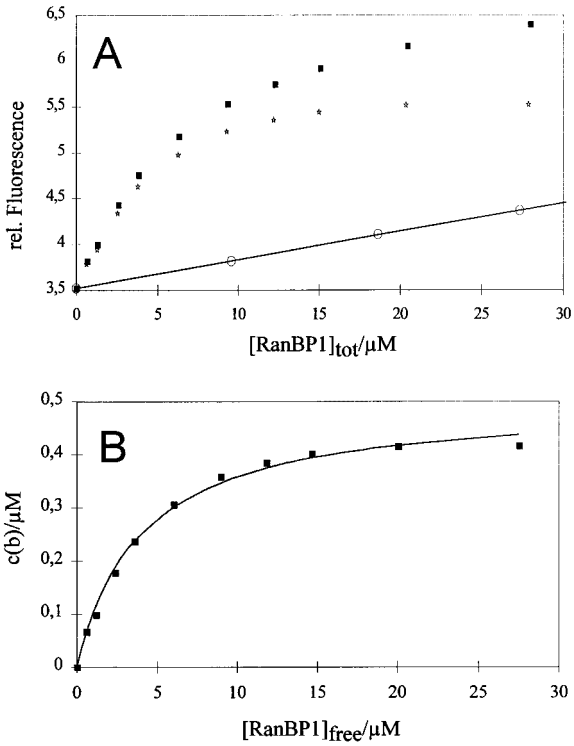

FIGURE 5: Increase in fluorescence signal on titration of RanBP1 into a solution of Ran·mdGDP. (A) Fluorescence emission (■) of 500 nM Ran·mdGDP (emission wavelength, 450 nm; excitation wavelength 350 nm) titrated with increasing amounts of RanBP1. Dilution of Ran was prevented by adding equal volumes of 1 μM Ran·mdGDP. The specific change in the fluorescence signal (☆) was calculated by subtraction of the fluorescence signal obtained upon addition of RanBP1 to buffer alone (○). Buffer: 20 mM KP_i, pH 7.5, 5 mM $MgCl_2$, and 1 mM β-mercaptoethanol, 20 °C. (B) Binding curve. Specific changes in the fluorescence signal were transformed to obtain concentrations of the Ran−RanBP1 complex. Data were fitted according to a 1:1 stoichiometry model by using SCIENTIST v2.0, resulting in a dissociation constant of 4.0 μM.

Table 3: Comparison between K_D Values for the Ran−RanBP1 Interaction Measured by Fluorescence Kinetics and Fluorescence Titration[a]

Ran	nucleotide	K_D (k_{on}/k_{off})	K_D (equilibria) (μM)
Ran(full-length)	mGppNHp	0.6 nM[a]	
Ran(full-length)	2′d3′mGDP	4.6 μM[b]	4.0 μM
RanΔC	mGppNHp	2.5 μM[a]	4.8 μM
		2.2 μM[b]	

[a] All experiments were performed in KP_i buffer. k_{off} was determined either in a competition experiment as described in Figure 3[b] or from ordinate value of k_{obs} vs [RanBP1] plots[c].

to the dextran matrix. These antibodies bind GST fusion proteins via the GST moiety, allowing the fusion partner (e.g., RanBP1) of the protein to be fully accessible in solution. Our investigations showed that GST fusion proteins bound by this method were fixed in a covalent-like manner to the surface matrix while regeneration with 20 mM glycine, pH 2, and 0.005% SDS resulted in complete dissociation of all noncovalently bound ligands, leaving the immobilized immunoglobulin with approximately full binding activity.

Figure 6A shows binding of Ran·GppNHp to binary complexes of antibody and GST−RanBP1 at different concentrations of Ran. Using BIAlogue 2.1 evaluation software, k_{obs} values for each experiment could be calculated, leading to association rates for the second-order reactions (Figure 6B). Dissociation rate constants were computed from

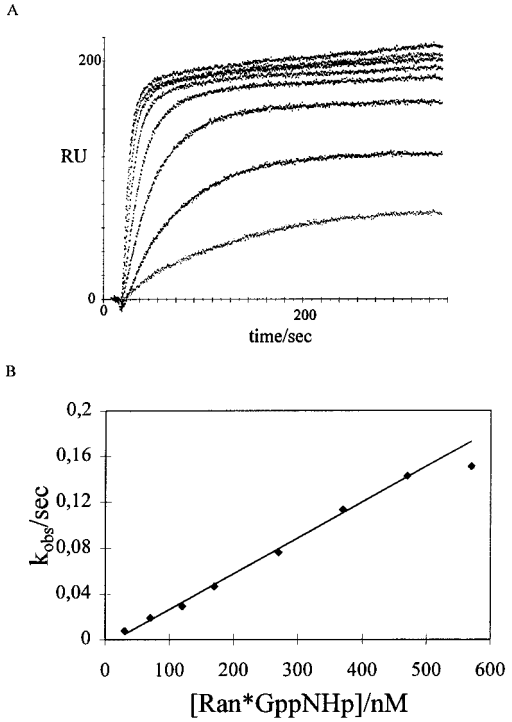

FIGURE 6: (A) Association of Ran·GppNHp to immobilized GST−RanBP1 protein. Anti-GST antibodies were covalently coupled to the surface of a BIAcore sensor chip. This antibody matrix was used to capture GST−RanBP1 in a quasi-irreversible manner. Injection of Ran·GppNHp in a concentration range from 30 to 600 nM could be followed by an increase in the resonance signal. Experiments were performed at 20 °C and in 10 mM HEPES, pH 7.4, 5 mM $MgCl_2$, and 0.0005% (w/v) Igepal. (B) Analysis of Ran·GppNHp interaction with GST−RanBP1 in SPR. To analyze the association reaction, BIAevaluation 2.1 software was used, yielding k_{obs} values for the individual Ran·GppNHp concentrations. Linear regression resulted in a k_{on} value of 3.5×10^8 M s^{-1}.

Table 4: Kinetic and Equilibria Constants for the Interaction between Ran(WT,fl) and GST−RanBP1 Obtained by Fluorescence and SPR Techniques at 20 °C in HEPES Buffer

technique	nucleotide	k_{on} [(M·s) × 10^{-5}]	k_{off} (×10^4 s)	K_D/nM
SPR	GppNHp	2.9; 3.1	3.7 ± 1.0, $n = 4$	1.2
SPR	mGppNHp	3.5	7.6 ± 1.3, $n = 6$	2.2
fluorescence	mGppNHp	3.0	10.5 ± 1.1, $n = 4$	3.5

long-term dissociation experiments of Ran protein from GST−RanBP1 by a single exponential fit. Table 4 gives an overview on kinetic data ascertained by fluorescence and SPR techniques.

Comparison between Biophysical Data Obtained by Fluorescence and SPR Measurements. No significant differences were found between k_{on} and k_{off} values determined by fluorescence or SPR techniques using the same reactants and buffer systems. While Ran·GppNHp exhibits the same association rate constant as Ran·mGppNHp in both assays, the dissociation rate is reduced by a factor of 2. This may indicate small disturbances in the interaction surface between Ran and the RanBP1 moiety by the mant group. The dissociation rate constant of Ran·mGppNHp measured by SPR is somewhat lower than that from fluorescence. The source of error using the SPR system could be that the dissociation rates may be inherent underestimations due to the rebinding of dissociated ligand to binding sites downstream in direction to the solvent flow (Nieba et al., 1996; O'Shannessy & Winzor, 1994). In order to prevent rebinding, we performed both dissociation experiments with different flow rates and in the presence of free RanBP1 to complex Ran·GppNHp directly after separation from GST−RanBP1. In both cases no changes in k_{off} were detected (data not shown). It should be stressed that slow off-rates in the BIAcore are often correlated with complex kinetic patterns due to surface adsorbtion of ligand and other matrix effects. Using an anti-GST serum to bind GST fusion proteins, we observed additional nonspecific binding of Ran protein to the antibody matrix, which was minimized by complete saturation of antibodies by GST proteins. Restrictions of the SPR technique for fast association reactions have been demonstrated recently (Hall et al., 1994). The association rate constants for the Ran/RanBP1 system as determined here are clearly within the limits of the BIAcore system.

Circular Dichroism. Circular dichroism spectra of proteins yield information about secondary structure composition. CD signals offer a linear correlation with substrate concentration. This can be demonstrated by comparing CD spectra which have been measured directly and those calculated using spectra measured at lower concentrations.

Here, circular dichroism spectra were measured for Ran·GDP, Ran·GppNHp, and RanBP1 alone and for the stochiometric mixtures of Ran·GDP or Ran·GppNHp and RanBP1. Figure 7A shows CD spectra of 2 and 4 μM Ran·GppNHp and the calculated 4 μM spectrum (2 times 2 μM spectrum). The calculated and measured spectra for 4 μM Ran·GppNHp are nearly identical, indicating true additivity of CD signals in the measured concentration range. The same is true for CD spectra of 2 and 4 μM RanBP1 (Figure 7B) and the same concentrations of Ran·GDP (data not shown).

Stoichiometric mixtures of Ran·GDP and RanBP1 produced the same CD spectra as calculated by the addition of the individual single spectra alone (Figure 7C). In contrast, there is a distinct difference between calculated (single components alone) and measured CD spectra of Ran·GppNHp and RanBP1 (Figure 7D). Due to the fact that CD spectra reflect secondary structure distribution in proteins, these changes indicate significant conformational changes upon complex formation between Ran·GTP and RanBP1.

DISCUSSION

The GTP-binding protein Ran is one of the main players in nucleo−cytoplasmic transport. Disturbances in the Ran pathway result in a broad pattern of different defects concerning protein import, the nuclear skeleton, RNA processing, and RNA transport and the cell cycle (Sazer, 1996). In particular, the function of Ran in protein import has become the object of numerous investigations. In analogy to Ras and other Ras-related proteins, several proteins exist which recognize Ran preferentially in its GTP-bound state and are potential effectors of Ras. These include RanBP1, RanBP2, and several sequence-related proteins with apparently similar folds (Hartmann & Görlich, 1995). A second type of Ran effector is importin-β (karyopherin-β), which together with importin-α is sufficient to bind nuclear localization signal (NLS) containing proteins to the nuclear pore (Floer & Blobel, 1996; Rexach & Blobel, 1994). While RanBP1 and RanBP2 binding to Ran is mutually exclusive, importin-β and RanBP1 have been shown to bind to Ran simultaneously (Chi et al., 1996). While Ras·GTP is thought to bind to and activate effector proteins like the protein kinase

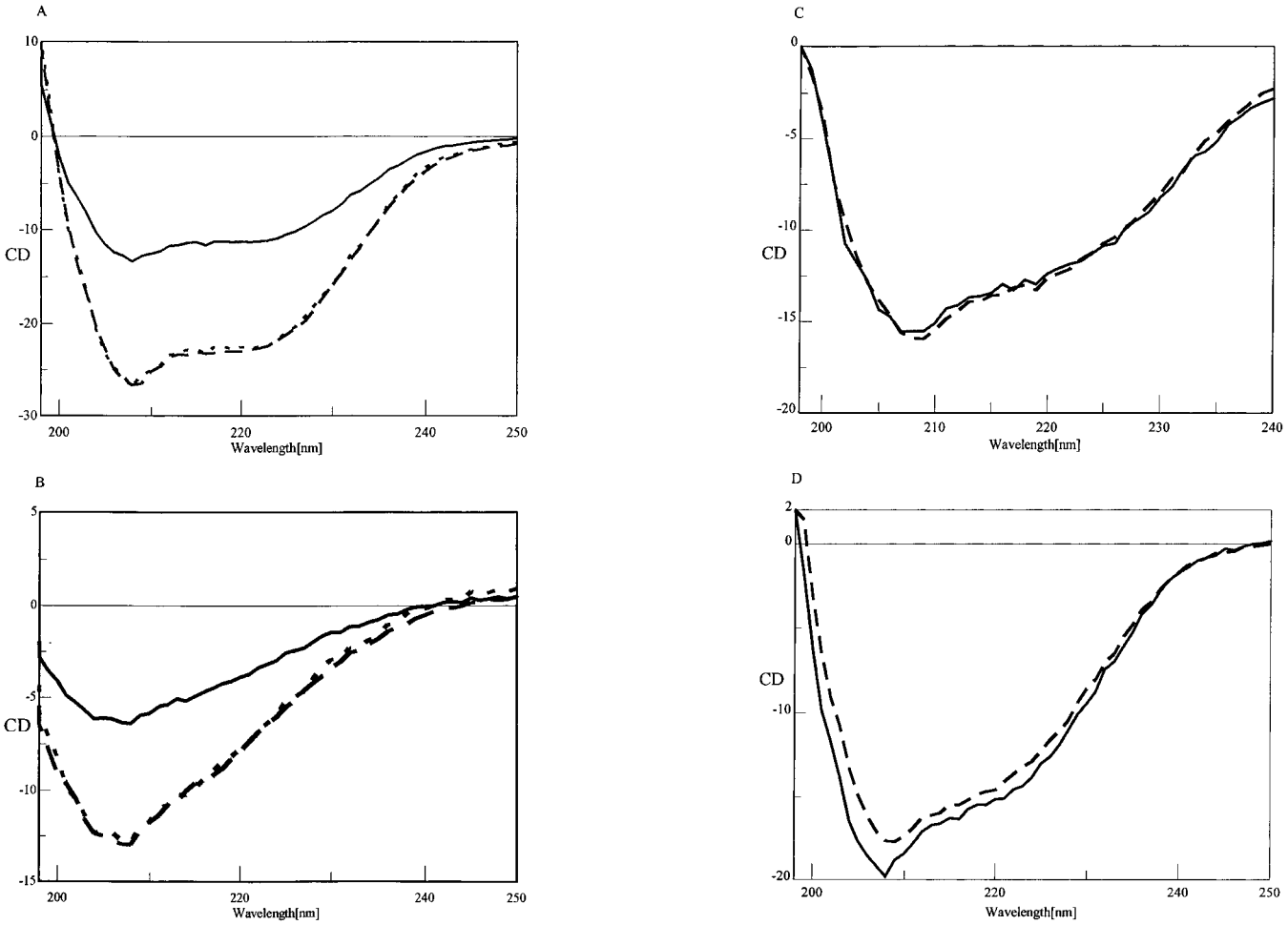

FIGURE 7: CD spectra of Ran·GppNHp (A), RanBP1 (B), mixtures of Ran·GDP and RanBP1 (C), and Ran·GppNHp·RanBP1 complex (D). Circular dichroism spectra of 2 and 4 μM solutions of Ran·GppNHp, Ran·GDP, and RanBP1 were measured in a Jasco J710 at 20 °C. Concentrations of Ran protein were calculated based on nucleotide concentrations. Spectra were base line corrected (− buffer spectra) and netto signals for 2 μM solutions multiplied by a factor of 2. Panels A and B show spectra of 2 μM (—), 4 μM (- - -), and 2 times 2 μM (···) of Ran·GppNHp and RanBP1, respectively. While a mixture of 2 μM Ran·GDP and 2 μM RanBP1 exhibits no difference between measured (- - -) and calculated (—) spectra (C), complex formation of 2 μM Ran·GppNHp with 2 μM RanBP1 results in a change in the CD signal (- - -) compared with the calculated sum spectra (—) as shown in panel D.

Raf, the role of Ran-binding proteins is much less clear. Their function in the nuclear pore complex (NPC) may be to organize Ran·GTP along the nuclear pore, where it may provide energy for vectorial transport by GTP hydrolysis.

Binding Affinities of the Ran−RanBP1 System. Using two independent methods, we obtained approximately identical values for rate constants and equilibria of the Ran−RanBP1 interaction. The binding affinity of the Ran·GTP−RanBP1 complex is in the nanomolar range, demonstrating highly specific recognition. It is about 20 times higher than the corresponding Ras·GTP−Raf^{RBD} (Ras-binding domain of the human Raf-1 protein kinase) interaction (Block et al., 1996). Comparable low K_D values were found for the interaction between Ran in its GTP-bound state and the Ran-binding domains of RanBP2 (Villa-Brazlavsky et al., unpublished results). It should be pointed out that Lounsbury et al. (1994) gave a first estimation of the Ran·GTP−RanBP1 affinity of 0.1 nM on the basis of overlay assays using Western blots on nitrocellulose. Recently Görlich et al. measured a K_I of 0.13 nM for the Ran·GTP−RanBP1 interaction by measuring the inhibition of RCC1-catalyzed GTP exchange on Ran·GTP by RanBP1 (Görlich et al., 1996).

Switching to the GDP-bound state of Ran or truncation of the C-terminus decreases the affinity of Ran toward RanBP1 dramatically by about four orders of magnitude. The resulting affinities of about 10 μM for the Ran·GDP·RanBP1 interaction or the RanΔC·GTP·RanBP1 interaction appear rather weak. Nevertheless, K_D values of about 10 μM were found for the interaction between p21^{Ras}·GppNHp and the catalytic domain of its GTPase-activating protein p120^{GAP} (Brownbridge et al., 1993; Eccleston et al., 1993) and Ran·GDP or Ran·GTP and RCC1 (Klebe et al., 1995b). Depending on the local concentration of Ran·GDP at the nuclear pore, functionally significant interactions with RanBP1 cannot be excluded.

Dynamic Aspects. The reduced affinity of Ran·GDP toward RanBP1 is caused by a 10-fold decrease of the association rate constant k_{on}, and an 1000-fold increase of the dissociation rate constant k_{off}. This indicates that the initial recognition of RanBP1 by Ran may not necessarily require the GTP-bound conformation, which is only required for formation of the tightly bound complex. These findings may supply a rationale for the observation that Ran·GDP forms a high-affinity ternary complex with RanBP1 in the presence of importin-β, while binary complexes between Ran·GDP and either RanBP1 or importin-β alone could not be demonstrated (Chi et al., 1996). The association rate constant of RanBP1 toward Ran·GDP is only modestly

reduced as compared with Ran·GTP. Therefore, binding of RanBP1 towards Ran·GDP is still a fast process and may be the initial reaction in the formation of a ternary complex, with importin-β recognizing and stabilizing the initial weak complex.

In contrast to the nucleotide effect on RanBP1 binding, truncation of the C-terminal acidic end of Ran results in both a 100-fold decrease of k_{on} and a similar increase of k_{off}. This suggests that the C-terminal DEDDDL sequence of Ran is involved in both the initial binding of RanBP1 and the stabilization of the complex. It may act as an initial recognition motif for RanBP1, while tight binding of RanBP1 is achieved via regions of the Ran protein that are sensitive to the nucleotide state of the protein.

Comparison between Fluorescence- and SPR-Based Experiments. Only limited data are available on the comparison of protein−protein interaction data obtained by the SPR technique and a second independent biophysical method (Vandermerwe & Barclay, 1996). Neri et al. compared the affinities of a synthetic single-chain antibody (scFvD1.3) toward lysozyme by fluorescence quenching and BIAcore measurements and got a K_a of 3.0×10^8 M^{-1} in the BIAcore system and 1.5×10^8 M^{-1} in the fluorescence experiment (Neri et al., 1995).

In our study, we could obtain and compare both dynamic and equilibria data from SPR and fluorescence measurements. Equilibrium and kinetic measurements of the Ran/RanBP1 interaction were made either in solution with fluorescence using analogues of guanine nucleotides or with surface plasmon resonance in a BIAcore system with the GST fusion protein of RanBP1 (GST−RanBP1) bound to a dextran matrix via anti-GST antibodies. To compare both systems, the same reactants (Ran·mGppNHp, GST−RanBP1) had to be tested in fluorescence and SPR assays. In our case, we could show that under the same conditions kinetic and equlibrium parameters for the interaction were identical within the standard errors of both methods.

This result is not obvious nor can it be expected for all comparable biophysical problems. The main difference between SPR and reactions in solution is the occurrence of additional matrix effects in the SPR system. Ligands may bind in a nonspecific manner toward the carboxylated dextran matrix of the sensor chip or to the covalently immobilized antibodies. This effect could only be observed for higher concentrations of Ran. Furthermore, the determination of the rate constants for the association reaction is limited by the diffusion of ligands from the fluid phase toward the sensor surface, while dissociation rate constants may be underestimated due to rebinding of dissociated ligand toward a binding partner located downstream in the binding lane. Additional problems may arise if the first reactant (GST−RanBP1 in our case) is not immobilized covalently, but bound via an anti-GST serum. In such cases, the slow dissociation of GST−RanBP1 from the matrix has to be considered at least in long-term experiments.

Nevertheless, the SPR technique opens an additional approach toward analysis of protein−protein interactions in particular when no other spectroscopic readout for the interaction is available. It would be helpful to have more data on the comparison between SPR and other biophysical methods using the same components to better weigh the advantages and pitfalls of the SPR technique. Here we found a remarkable agreement between the two different data sets.

Structural Considerations. The three-dimensional structure of Ran·GDP as described by Scheffzek et al. (1995) exhibits significant variations in regions involved in GDP and Mg^{2+} coordination compared to that of Ras. As a consequence, considerable conformational changes would be necessary to reorganize the Ran G-domain upon binding of GTP such that the elements thought to be universal for the molecular switch resemble those found in other G domains bound to GTP. Studies on the crystal structure of EF-Tu complexed with GDP showed an unexpected structural homology in the effector region with Ran·GDP (Polekhina et al., 1996; Abel et al., 1996). In EF-Tu, the change from EF-Tu·GTP to EF-Tu·GDP is coupled with a switch from α-helical to β-sheet in the secondary structure of the switch I region. If the homology between Ran and EF-Tu is true for the GTP-bound state too, considerable changes in tertiary and secondary structure should be expected for the transition from Ran·GDP toward Ran·GTP.

The CD spectra of Ran·GDP and Ran·GppNHp did not show relevant differences in secondary structure. On the other hand, CD spectra of Ran·GppNHp·RanBP1 indicate significant changes of the secondary structure of the participating proteins upon forming the complex. So far, we cannot discriminate if the changes in secondary structure on complex formation take place in Ran or RanBP1 alone, or in both proteins together. Possibly the CD data may indicate that conformational changes in the G-domain of Ran similar to those observed for the EF-Tu·GTP → EF-Tu·GDP transition may require the interaction with another protein, such as RanBP1.

ACKNOWLEDGMENT

We thank Christine Nowak for excellent technical assistance, Jörg Becker and Rohit Mittal for reviewing the manuscript, and Jürgen Huber for programming the fluorescence titration device.

REFERENCES

Abel, K., Yoder, M. D., Hilgenfeld, R., & Jurnak, F. (1996) *Structure 4*, 1153.
Beddow, A. L., Richards, S. A., Orem, N. R., & Macara, I. G. (1995) *Proc. Natl. Acad. Sci. U.S.A. 92*, 3328.
Bischoff, F. R., Klebe, C., Kretschmer, J., Wittinghofer, A., & Ponstingl, H. (1994) *Proc. Natl. Acad. Sci. U.S.A. 91*, 2587.
Bischoff, F. R., Krebber, H., Smirnova, E., Dong, W., & Ponstingl, H. (1995) *EMBO J. 14*, 705.
Block, C., Janknecht, R., Herrmann, C., Nassar, N., & Wittinghofer, A. (1996) *Nat. Struct. Biol. 3*, 244.
Bradford, M. M. (1976) *Analytical Biochemistry 72*, 248.
Bressan, A., Somma M. P., Lewis, J., Santolamazza, C., Copeland, N. G., Gilbert, D. J., Jenkins, N. A., & Lavia, P. (1994) *Gene 103*, 201.
Brownbridge, G. G., Lowe, P. N., Moore, K. J., Skinner, R. H., & Webb, M. R. (1993) *J. Biol. Chem. 268*, 10914.
Chaiken, I., Rose, S., & Karlsson, R. (1992) *Anal. Biochem. 201*, 197.
Chi, N. C., Adam, E. J. H., Visser, G. D., & Adam, S. A. (1996) *J. Cell Biol. 135*, 559.
Coutavas, E., Ren, M., Oppenheim, J. D., D'Eustachio, P., & Rush, M. G. (1993) *Nature 366*, 585.
Eccleston, J. F., Moore, K. J., Morgan, L., Skinner, R. H., & Lowe, P. N. (1993) *J. Biol. Chem. 268*, 27012.
Floer, M., & Blobel, G. (1996) *J. Biol. Chem. 271*, 5313.
Gershon, P. D., & Khilko, S. (1995) *J. Immunol. Methods 183*, 65.
Görlich, D., & Mattaj, I. W. (1996) *Science 271*, 1513.
Görlich, D., Pante, N., Kutay, U., Aebi, U., & Bischoff, F. R. (1996) *EMBO J. 15*, 5584.

Gutfreund, H. (1995) *Kinetics for the Life Sciences*, Cambridge University Press; Cambridge, U.K.
Hall, D. R., Cann, J. R., & Winzor, D. J. (1994) *Anal. Biochem. 235*, 175.
Hartmann, E., & Görlich, D. (1995) *Trends Cell Biol. 5*, 192.
Hiratsuka, T. (1983) *Biochim. Biophys. Acta 742*, 496.
John, J., Sohmen, R., Feuerstein, J., Linke, R., Wittinghofer, A., & Goody, R. S. (1990) *Biochemistry 29*, 6058.
Klebe, C., Nishimoto, T., & Wittinghofer, F. (1993) *Biochemistry 32*, 11923.
Klebe, C., Bischoff, F. R., Ponstingl, H., & Wittinghofer, A. (1995a) *Biochemistry 34*, 639.
Klebe, C., Prinz, H., Wittinghofer, A., & Goody, R. S. (1995b) *Biochemistry 34*, 12543.
Kornbluth, S., Dasso, M., & Newport, J. (1994) *J. Cell Biol. 125*, 705.
Lounsbury, K. M., Beddow, A. L., & Macara, I. G. (1994) *J. Biol. Chem. 269*, 11285.
Macara, I. G., Lounsbury, K. M., Richards, S. A., Mckiernan, C., & Barsagi, D. (1996) *FASEB J. 10*, 625.
Malmborg, A. C., Michaelsson, A., Ohlin, M., Jansson, B., & Borrebaeck, C. A. (1992) *Scand. J. Immunol. 35*, 643.
Melchior, F., Guan, T. L., Yokoyama, N., & Nishimoto, T. (1995) *J. Cell Biol. 131*, 571.
Moore, M. S., & Blobel, G. (1994) *Trends Biochem. Sci. 19*, 211.
Neri, D., Momo, M., Prospero, T., & Winter, G. (1995) *J. Mol. Biol. 246*, 367.
Nieba, L., Krebber, A., & Pluckthun, A. (1996) *Anal. Biochem. 234*, 155.
O'Shannessy, D. J., & Winzor, D. J. (1996) *Anal. Biochem. 236*, 275.
O'Shannessy, D. J., Brigham-Burke, M., & Peck, K. (1992) *Anal. Biochem. 205*, 132.
Polekhina, G., Thirup, S., Kjeldgaard, M., Nissen, P., Lippmann, C., & Nyborg, J. (1996) *Structure 4*, 1141.
Ren, M., Coutavas, E., D'Eustachio, P., & Rush, M. G. (1994) *Mol. Cell. Biol. 14*, 4216.
Ren, M., Villamarin, A., Shih, A., Coutavas, E., Moore, M. S., LoCurcio, M., Clarke, V., Oppenheim, J. D., D'Eustachio, P., & Rush, M. G. (1995) *Mol. Cell. Biol. 15*, 2117.
Rexach, M., & Blobel, G. (1994) *Cell 83* (5), 683.
Rush, M. G., Drivas, G., & Deustachio, P. (1996) *Bioessays 18*, 103.
Sazer, S. (1996) *Trends Cell Biol. 6*, 81.
Scheffzek, K., Klebe, C., Fritz-Wolf, K., Kabsch, W., & Wittinghofer, A. (1995) *Nature 374*, 378.
Schlenstedt, G. (1996) *FEBS Lett. 389*, 75.
VanCott, T. C., Loomis, L. D., Redfield, R. R., & Birx, D. L. (1992) *J. Immunol. Methods 146*, 163.
Vandermerwe, P. A., & Barclay, A. N. (1996) *Curr. Opin. Immunol. 8*, 257.
Yokoyama, N., Hayashi, N., Seki, T., Panté, N., Ohba, T., Nishii, K., Kuma, K., Hayashida, T., Miyata, T., Aebi, U., Fukui, M., & Nishimoto, T. (1995) *Nature 376*, 184.

BI970524K